TECHNISCHE HOGESCHOOL VLIEGTUIGBOUWKUNDE

Report V.T.H.-74.

A suggested semi-empirical method for the calculation of the boundary layer transition region.

by

J. L. van Ingen

Delft - Nederland

September 1956

A SUGGESTED SEMI-EMPIRICAL METHOD FOR THE CALCULATION OF THE BOUNDARY LAYER TRANSITION REGION. [+]

by J.L.van Ingen [++]

Summary

The suggested method will be restricted to incompressible two-dimensional flow and is based on the theory of boundary layer stability, which is due to Tollmien, Schlichting and other investigators.

For the flat plate the amplification of unstable oscillations in the laminar boundary layer was calculated. The results of this calculation were compared with the experimental determination of the transition region. It was found that at the beginning of the transition region the amplitude of the oscillations with maximum amplification is $e^{7,8}$ (≈2500) times the amplitude of the neutral oscillations.

In some cases for the airfoil section EC 1440 the same amplification ratio at transition was found as for the flat plate. In other cases, however, differences exist between the results for the flat plate and for the airfoil section. These differences may be caused by lack of sufficient numerical results of the stability theory (section 2).

Therefore it seems possible to calculate the position of the transition region for an airfoil section by calculating the amplification of unstable oscillations and assuming that transition begins as soon as the amplification ratio has reached the value $e^{7,8}$. For this calculation only the pressure distribution has to be known.

From the stability theory only the relation between the amplitude of the oscillations at a given moment and the amplitude at the beginning of the unstable region is found. Therefore the actual magnitude of the oscillations cannot be calculated, the magnitude at the beginning of the unstable region being unknown.

[+]) Communication presented at the Second European Aeronautical Congress, Scheveningen, Netherlands, September 25th-29th, 1956.

[++]) Department of Aeronautical Engineering, Technological University, Delft.

In this paper it will be shown, that knowledge of the amplification ratio is probably sufficient for the suggested semi-empirical method. It is not quite clear why the actual magnitude of the amplitude should not be important; possibly the initial amplitudes where about the same in all cases because of equal stream turbulence, surface roughness etc.

The described investigations, of which a more complete account is given in [1] , cannot be considered as conclusive, as only a few cases have been analysed.

List of Symbols

a amplitude of oscillation.

c airfoil chord.

c_r $\frac{\beta_r}{\alpha}$

c_i $\frac{\beta_i}{\alpha}$

f oscillation frequency.

R_x x-Reynolds number for flat plate. $(\frac{U.x}{\nu})$

R chord- Reynolds number for airfoil section. $(\frac{V.c}{\nu})$

R_δ Reynolds number, based on displacement thickness. $(\frac{U.\delta^*}{\nu})$

s distance to leading-edge of airfoil section, measured along contour.

t time.

U velocity at outer edge boundary layer.

V wind velocity

x distance to leading-edge of flat plate; also: distance to leading-edge of airfoil section (measured along chord).

α angle of incidence; also $\frac{2\pi}{\lambda}$.

λ wave length; also velocity-profile-shape parameter according to Pohlhausen.

β velocity-profile-shape parameter according to Hartree.

β_i amplification coefficient.

β_r $2\pi f$

δ^* displacement thickness.

ν kinematic viscosity.

σ amplification factor $\int_{t_o}^{t} \beta_i dt$; amplification ratio=ratio of amplitudes of oscillation at times t and t_o $= e^{\sigma}$.

suffix o refers to conditions at beginning of unstable region.

1. Introduction

Although the knowledge of the mechanics of boundary layer transition, is rather extensive [2,3,4,5], it has not been possible to calculate the position of the transition region by pure theoretical methods.

The existing theory concerning the instability of the laminar boundary layer, in which is shown that small disturbances may grow and thus cause transition, ([6], chapter XVI) is a linear one and thus cannot describe the transition process completely. For this reason it is necessary to rely on semi-empirical methods for the calculation of the transition region position, which has to be known for the calculation of profile drag.

These semi-empirical methods should take into account all the factors which influence the transition. Such factors are: shape of the boundary layer velocity profile and the Reynolds number $R_{\delta}*$ (which depend on the pressure distribution); free stream turbulence and surface roughness. Turbulence and surface roughness may be neglected if they are sufficiently small.

Semi-empirical methods based on $R_{\delta}*$ alone are not universally valid. In [7] e.g. it is shown that transition on an NACA $65_{(215)}$-114 airfoil section begins, as soon as the Reynolds number $\frac{U.\delta_{0,707}}{\nu}$ has reached the value 8000; $\delta_{0,707}$ being the distance from the wall to the point in the boundary layer where the velocity equals 0,707 U. For the simple case of the boundary layer along a flat plate $\frac{U.\delta_{0,707}}{\nu}$ = 8000 corresponds to $R_{\delta}* = 5850$. From experiments [2] it is known, however, that transition of the flat-plate boundary layer begins at $R_x = 2{,}80 \times 10^6$, which is equivalent to $R_{\delta}* = 2900$. This value does not agree with the value 5850 mentioned for the NACA $65_{(215)}$- 114 section.

In the present paper it will be shown that a semi-empirical method, based on stability theory gives a better correlation between transition on the flat plate and on an airfoil section. Although stability theory is not valid near the transition region due to the linearisation, it might be a sound basis for developing a semi-empirical method.

In the suggested method the stability theory will be used to combine important factors as shape of the velocity profile and Reynolds number distribution into one single parameter σ, which determines the amplification of unstable oscillations.

This amplification factor will be calculated for the boundary layer along a flat plate and on the EC 1440 airfoil section. By comparing the results of these calculations with the results of transition measurements the value of the amplification factor at which transition occurs can be found. If this factor would have the same value in all cases, it can be used to calculate the transition region position, by assuming that transition begins, as soon as the calculated amplification ratio has reached this specific value.

2. Stability theory

In this section a short description of the stability theory will be given. A detailed survey can be found in [2], chapter XVI.

In the stability theory a given laminar main flow is subjected to small disturbances of which the amplification or damping can be calculated. The stability depends on such factors as: shape of the velocity profile and Reynolds number $R_{\delta^*} = \frac{U.\delta^*}{\nu}$ (which depend on the pressure distribution) and wave length or frequency of the disturbances.

In stability theory a periodic disturbance is assumed with stream function:

$$\psi = \varphi(y)\, e^{i(\alpha x - \beta t)} \qquad (1)$$

where $\varphi(y)$ represents the initial amplitude, depending only on y; $\alpha = \frac{2\pi}{\lambda}$ where λ is the wave length and t is the time. Since β is generally a complex quantity $= \beta_r + i\beta_i$ (1) may be written:

$$\psi = \varphi(y)\, e^{\beta_i t}\, e^{\,i(\alpha x - \beta_r t)} \qquad (2)$$

$\beta_r = 2\pi f$ where f is the frequency; β_i is the coefficient of amplification or damping, depending on whether it is positive or negative. The wave velocity is equal to $c_r = \frac{\beta_r}{\alpha}$.

From (2) it can be found that the relation between the amplitudes a_o and a of ψ at times t_o and t is given by:

$$\frac{a}{a_o} = e^{\int_{t_o}^{t} \beta_i \, dt} \qquad (3)$$

The same relation can be shown to hold for the disturbance velocities.

The quantity $\int_{t_o}^{t} \beta_i dt$ will be called the amplification factor σ (t_o is the time at which the disturbance enters the unstable region).

The amplification ratio is then equal to $\frac{a}{a_o} = e^{\sigma}$. With $c_r = \frac{ds}{dt}$ the expression for σ can be written as $\sigma = \int_{s_o}^{s} \frac{\beta_i}{c_r} ds$ and can be calculated for oscillations of different frequencies β_r as soon as $\frac{\beta_i}{c_r}$ is known as a function of s.

To find $\frac{\beta_i}{c_r}$ for a given value of s, it is necessary to obtain numerical results of stability theory for the boundary layer velocity profile at that station. This work, which is very labourious, was done by Pretsch for the Hartree velocity profiles; [8] and [9]. For the velocity profiles of the method of Pohlhausen, however, which was used in this paper for the calculation of the laminar boundary layer no complete stability calculations are available. Therefore the results of Pretsch have been used for the calculation of σ by transferring the stability characteristics of the Hartree profiles to the Pohlhausen profiles.

The relation between the shape parameters λ and β of the Pohlhausen and Hartree profiles, which can be used for this purpose, according to [8], is shown in fig.1. This relation cannot be completely right, however, due to the fact that the separation profiles $\lambda = -12$ and $\beta = -0{,}198$ of the two families don't match.

The value $\beta = -0{,}198$ is reached for $\lambda = -7$ already, so that at small values of λ the value of β from fig.1 is too low. As the instability increases as λ decreases, the calculated instability will be too high for negative values of λ. For positive values of λ and β the correspondence is better; $\lambda = 7{,}052$ corresponds exactly with $\beta = 1$, which give the stagnation profiles. The abovementioned inaccuracy in the λ-β relation will be the cause of certain discrepancies in the results of the calculations, described in section 4.

The calculation of the amplification of unstable disturbances is performed as follows. From measurements or calculations the velocity U is known as a function of the co-ordinate s. The boundary layer calculations give the values of δ^*, R_{δ^*} and velocity profile shape parameter (= λ for the Pohlhausen method which is used in this paper) With the aid of fig.1 and the results of [9] it is then possible to find, for different values of the reduced frequency $\frac{\beta_r \nu}{U^2}$ the values of $\frac{\beta_i \delta^*}{U}$ and $\alpha\delta^*$ as a function of s. The amplification factor $\sigma = \int_{t_o}^{t} \beta_i dt$ can then be calculated with:

$$\sigma = \int_{t_o}^{t} \beta_i \, dt = \int_{s_o}^{s} \frac{\beta_i}{c_r} \, ds = \int_{s_o}^{s} \frac{\beta_i \delta^*}{U} \cdot \frac{U}{c_r} \cdot \frac{1}{\delta^*} \, ds \qquad (4)$$

in which $\frac{U}{c_r}$ follows from:

$$\frac{c_r}{U} = \frac{\beta_r \nu}{U^2} \cdot \frac{1}{\alpha \delta^*} \cdot \frac{U \delta^*}{\nu} \qquad (5)$$

3. Determination of the maximum amplification factor at transition for the flat plate boundary layer.

As first case to be considered, the flat plate is chosen because results of accurate measurements are available for that case (fig.2 , taken from [2] .) Moreover the boundary layer flow along a flat plate is very simple as the shape of the velocity profile does not change with the distance x to the leading-edge.

Due to the fact that for the flat plate, U is independent of x, eq.(4) can be written for this case as:

$$\sigma = \int_{x_o}^{x} \frac{\beta_i}{c_r} \, dx = \int_{x_o}^{x} \frac{\beta_i \delta^*}{U} \cdot \frac{U}{c_r} \cdot \frac{\nu}{U \delta^*} \, d\left(\frac{Ux}{\nu}\right) = \int_{R_{x_o}}^{R_x} \frac{\beta_i \delta^*}{U} \cdot \frac{U}{c_r} \cdot \frac{1}{R_{\delta^*}} \, d(R_x) \qquad (6)$$

By aid of the results of [9] the quantity $\frac{\beta i \delta^*}{U} \cdot \frac{U}{c_r} \cdot \frac{1}{R_{\delta^*}}$ can be found as a function of R_{δ^*} , and as for the flat plate $R_{\delta^*} = 1{,}73\sqrt{R_x}$, this quantity is also known as a function of R_x. For different values of the reduced frequency $\frac{\beta_r \nu}{U^2}$ the result is shown in fig. 3. By integration according to (6) the amplificationfactor σ is found as a function of R_x (fig.4). From the figures 3 and 4 it can be seen, that for a disturbance with a given frequency the amplitude increases ($\beta_i > 0$) until a maximum is reached, then the disturbance becomes stable again and the amplitude decreases. ($\beta_i < 0$).

The envelope of the curves for σ from fig. 4 gives the maximum amplificationfactor σ_{max} as a function of R_x. The value of σ_{max} increases continuously from o at $R_x = 0{,}154.10^6$. Below this value of R_x there are no unstable oscillations; that means $R_x = 0{,}154 \times 10^6$,

which corresponds to $R_{\delta^*} = 680$, is the critical Reynolds number for the flat plate boundary layer.

For the calculation of the amplificationfactor the stability theory was used which is not valid at large amplifications. For the suggested method, however, this is not a serious draw-back, because the amplificationfactor is only used as a parameter in which several factors, which are known to be important for transition are correlated. It might be hoped that σ can be used as a basis for developing a semi-empirical method for the calculation of the boundary layer transition region.

According to linearised stability theory the amplified oscillations are still regular. From experiments it is known, however, that suddenly the irregular turbulent motion appears. According to fig. 2 the transition region begins at $R_x = 2{,}80 \times 10^6$ and ends at $R_x = 3{,}90 \times 10^6$ if the stream turbulence is less than about 0,08%, which is the case in the atmosphere and in modern low-speed wind tunnels. From fig. 4 it is seen, that the two mentioned values of R_x correspond with values 7,8 and 10 for the amplificationfactor. This means, that at the beginning and end of the transition region the amplitude of the oscillations is $e^{7,8} = 2500$ and $e^{10} = 22500$ times the amplitude at $R_x = 0{,}154 \times 10^6$. As for all flat plate experiments the same value of the x-Reynolds number for transition is found, the values 7,8 and 10 for the amplificationfactor at transition apply to all flat plate experiments.

If these values can be shown to be valid also for boundary layers with a pressure gradient, the position of the transition region can be calculated by assuming that transition begins as soon as the amplificationfactor has reached the value 7,8 and ends at a value of this factor equal to 10.

In the next section the amplificationfactor at transition for the boundary layer on an EC 1440 airfoil section will be calculated.

4. Determination of the maximum amplificationfactor at transition of the boundary layer on the EC 1440 airfoil section.

4.1. Measurements of transition region and pressure distribution and calculation of the laminar boundary layer.

In the low-turbulence windtunnel of the Aeronautical Department of the Technological University of Delft [10] the pressure - distribution and the transition region were measured for the EC 1440

airfoil section with 0,60 m chord at Reynolds numbers up to $4{,}35 \times 10^6$.

The transition region, which was measured with a small total-head tube on the surface of the model, is given in fig. 5 as a function of α for $R=4{,}35\times10^6$. The results for other values of the Reynolds number are similar.

The pressure distribution was measured by means of pressure holes in the model surface. From this pressure-distribution the velocity U at the edge of the boundary layer was found as a function of s.

The laminar boundary layer was calculated by the method of Pohlhausen ([6], chapter XII). The velocity U and the results of the boundary layer calculation (δ^* , $R_{\delta^*} = \frac{U\delta^*}{\nu}$, the velocity profile shape parameter λ and the critical Reynolds number $R_{\delta^*_{crit}}$) are shown as a function of the co-ordinate s for $\alpha=0^\circ$ at $R = 4{,}35 \times 10^6$ in fig. 6. The results for other values of α and R are similar.

4.2. Calculation of the maximum amplificationfactor at transition for $R = 4{,}35 \times 10^6$.

The amplificationfactor was calculated as described in section 2 The values of $\frac{\beta_i}{c_r}$ are shown in fig. 7 for $\alpha=0^\circ$. From this figure it is seen, that the instability becomes very large for negative values of λ , due to the negative pressure gradient over the rear part of the airfoil section.

The amplificationfactor for $\alpha=0^\circ$ is shown in fig.8. The envelope of the curves for different values of $\frac{\beta_r \nu}{U^2}$ gives the maximum amplificationfactor σ_{max} as a function of s. For the other values of α similar calculations were performed. From these calculations fig.9 has been composed in which curves for constant values of σ_{max} are drawn, together with the measured transition region of fig. 5.

The curve for $\sigma_{max}=0$ gives the position on the chord where the boundary layer becomes unstable. This instability point moves upstream as α is increased just as the transition region. Transition occurs at a great distance behind this instability-point, however. This means, the disturbances have to travel a long way before the amplification is large enough to cause transition.

Special attention should be given to the curves for $\sigma_{max}=7{,}8$ and 10, which for the flat plate boundary layer were shown to

correspond with the beginning and end of the transition region. If these values should also apply to airfoil sections, the curves for σ_{max} = 7,8 and 10 should coincide with the beginning and end of the transition region. For values of α near 0° a good correspondence is shown; for other values of α, however, differences exist. As a consequense, using the factors 7,8 and 10 for estimating the position of the transition region, the result would be somewhat in error. The magnitude of these errors is given in the upper part of table I for different values of α. The errors increase with α increasing or decreasing from zero.

In fig.10 the value of σ_{max} at the beginning of the transition region is plotted against the value of λ for all cases which have been analysed. From this figure it is seen, that σ_{max} generally increased when λ decreases, with the exception of the cases no 4 and 5 ($\alpha=+2^\circ$ and 3° for $R = 4{,}35 \times 10^6$).

Although it is not impossible, that σ_{max} at transition should depend on λ, it is more likely that the errors (except for $\alpha = +2^\circ$ and 3°) are caused by the inaccuracy of the relation between the shape parameters λ and β of the Pohlhausen and Hartree velocity profiles. (section 2). By this inaccuracy the instability is increased, so that a particular value of σ_{max} is reached for too small a value of x/c. This explains why the curves for σ_{max} = 7,8 and 10 lie too low for negative values of α in fig.9. To reduce these errors it is necessary to obtain a better relation between λ and β, or even to make such a relation superfluous by performing stability calculations for the same velocity profiles as are used in the boundary layer calculation.

For $\alpha = +2^\circ$ and $+3^\circ$ the differences between the curves for σ_{max} = 7,8 (10) and the beginning (end) of the measured transition region are rather large. This is caused for a great deal by inaccuracies in the calculation of the laminar boundary layer, which was performed by an approximation to Pohlhausen's method ([6], p 199). In this approximation the labourious process of numerically solving a differential equation is replaced by numerically evaluating a definite integral. This approximation might be invalid, however, for large values of α.

Also some measurements and calculations were performed for the EC 1440 airfoil section at lower Reynolds numbers, for $\alpha=0^\circ$. Due to the inaccuracy in the λ-β relation, mentioned above, no good agreement is found with the results for the flat plate, as is shown in the lower part of table I.

In order to reduce the errors in the calculation of σ_{max} for $\alpha = +2^0$ and 3^0 at $R = 4{,}35 \times 10^6$ the investigations are being refined by calculating the laminar boundary layer by the exact method of [11]. Preliminary results of these calculations show the distance between the curves for $\sigma_{max} = 7{,}8$ (10) and the beginning (end) of the transition region to be reduced to about half the values of fig. 9 and table I for positive α. For negative α, the recalculated positions of $\sigma_{max} = 7{,}8$ and 10 are nearly the same as before. This is due to the fact, that also in the improved calculation a relation similar to that of fig. 1, had to be used with the same type of inaccuracy.

It is not yet known, whether calculation of the laminar boundary layer by the exact method of Pohlhausen would have resulted in the same reduction of the errors in the position of $\sigma_{max} = 7{,}8$ and 10.

Conclusions.

1. For the boundary layer along a flat plate transition starts as soon as the calculated amplification ratio of unstable disturbances has reached the value $e^{7{,}8}$ (≈2500) and ends at an amplification ratio of e^{10} (≈22500).

2. For the EC 1440 airfoil section the same amplification ratio at transition has been found in some cases as for the flat plate. For other cases, no good agreement with the results for the flat plate has been obtained.

3. To improve the accuracy of the suggested semi-empirical method for the calculation of the boundary layer transition region, stability calculations should be performed for the same velocity profiles as are used for the boundary layer calculations. As the method of [11] is thought to be better than Pohlhausen's, especially in the region of retarded flow, it would be desirable to have such calculations performed for the velocity profiles of [11].

4. In order to make possible a final conclusion concerning the accuracy and usefulness of the suggested method, further investigations are required, especially at higher Reynolds numbers.

Acknowledgement.

The author is indebted to prof.dr. R. Timman of the Institute of Applied Mathematics, Technological University, Delft for several enlightening discussions during the course of this investigation and for the permission to have some calculations performed by the staff of that Institute.

References.

1. Van Ingen, J.L.: "Een semi-empirische methode voor de bepaling van de ligging van het omslaggebied van de grenslaag bij onsamendrukbare twee-dimensionale stromingen". Rep. VTH-71 of the Dept, of Aeron. Eng. Techn. University, Delft, 1956.

2. Schubauer, G.B. and Skramstad, H.K.: "Laminar-boundary-layer oscillations and transition on a flat plate", NACA Rep. 909, 1948.

3. Malotaux, P.C.A., Denier van der Gon, J.J. and Yap Kie Jan: "Methode voor kwalitatief grenslaagonderzoek met behulp van gloeidraden zonder beinvloeding van de stroming". Rep. VTH-45 of the Dept. of Aeron. Eng., Techn. University, Delft, 1951.

4. Schubauer, G.B. and Klebanoff, P.S.: "Contributions on the mechanics of boundary layer transition", NACA TN 3489, 1955.

5. Dryden, H.L.: "Transition from laminar to turbulent flow at subsonic and supersonic speeds", Proceedings of the conference on highspeed aeronautics. Polytech. Institute of Brooklyn, 1955, p. 41 - 74.

6. Schlichting, H.: "Grenzschichttheorie", Edited by G. Braun, Karlsruhe, 1951.

7. Braslow, A.L. and Visconti, F.: "Investigation of boundary-layer Reynoldsnumber for transition on an NACA 65 (215)-114 airfoil in the Langley two-dimensional low turbulence windtunnel", NACA TN 1704, 1948.

8. Pretsch, J.: "Die Stabilität einer ebenen Laminarströmung bei Druckgefälle und Druckanstieg", Jahrbuch 1941 der deutschen Luftfahrtforschung, p. 1 - 58.

9. Pretsch, J.: "Die Anfachung instabiler Störungen in einer laminaren Reibungsschicht". Jahrbuch 1942 der deutschen Luftfahrtforschung, p. 1 - 54.

10. Dobbinga, E. and van Ghesel Grothe, J.A.: "De lage snelheids windtunnel van de sub-afd. Vliegtuigbouwkunde der Technische Hogeschool". De Ingenieur, 23 Sept. 1955, p. A 461.

11. Timman, R.: "A one parameter method for the calculation of laminar boundary layers". N.L.L. rep. F 35, 1948.

Table I: Magnitude of the error Δx in the calculation of the transition region for the EC 1440 airfoil section. (all values are given in % chord; $\Delta x < 0$ denotes that the calculated transition region is found too far forward).

R	α	measured transition region		calculated transition region		error Δx	
	degrees	beginning	end	beginning (σ_{max}=7,8)	end (σ_{max}=10)	beginning	end
$4{,}35 \times 10^6$	0	50,5	57,5	50	53	- 0,5	- 4,5
	0,5	44,5	53	44,5	49	0	- 4
	1	37,5	47	37	42	- 0,5	- 5
	1,5	32	40,5	27,5	32	- 4,5	- 8,5
	2	27	34	16	18,5	-11	-15,5
	2,5	21,5	28	11	13	-10,5	-15
	3	17	21,5	9	10,5	- 8	-11
	-0,5	55	62	53	56	- 2	- 6
	-1	58,5	66	56	58	- 2,5	- 8
	-2	64	72	60	61,5	- 4	-10,5
	-3	68	-	62,5	63,5	- 5,5	-
	-4	72	-	64	65	- 8	-
$2{,}4 \times 10^6$	0	64	71	52	54,5	-12	-16,5
3×10^6	0	59	67	51	52,5	- 8	-14,5
$3{,}4 \times 10^6$	0	56	64	50	52	- 6	-12
4×10^6	0	52	60	50	52	- 2	- 8
$4{,}35 \times 10^6$	0	50,5	57,5	50	53	- 0,5	- 4,5

If the boundary layer calculation is refined, the values of Δx for $\alpha > 0^0$ may be reduced to about half the value given in the table. (see page 10).

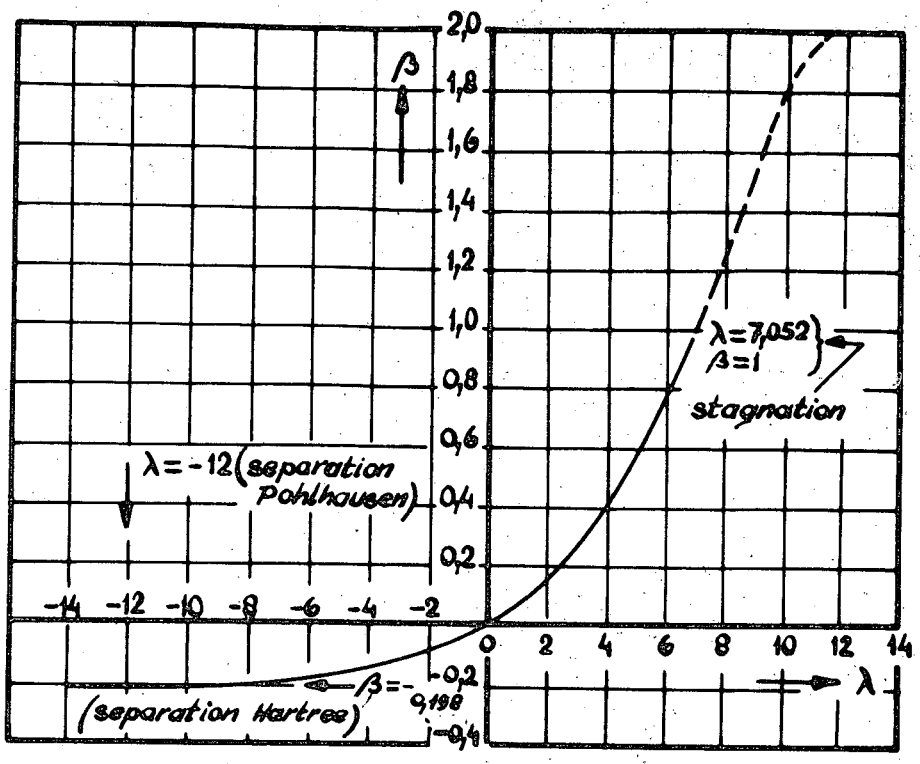

Fig.1: Relation between shape parameters λ and β of Pohlhausen and Hartree velocity profiles.

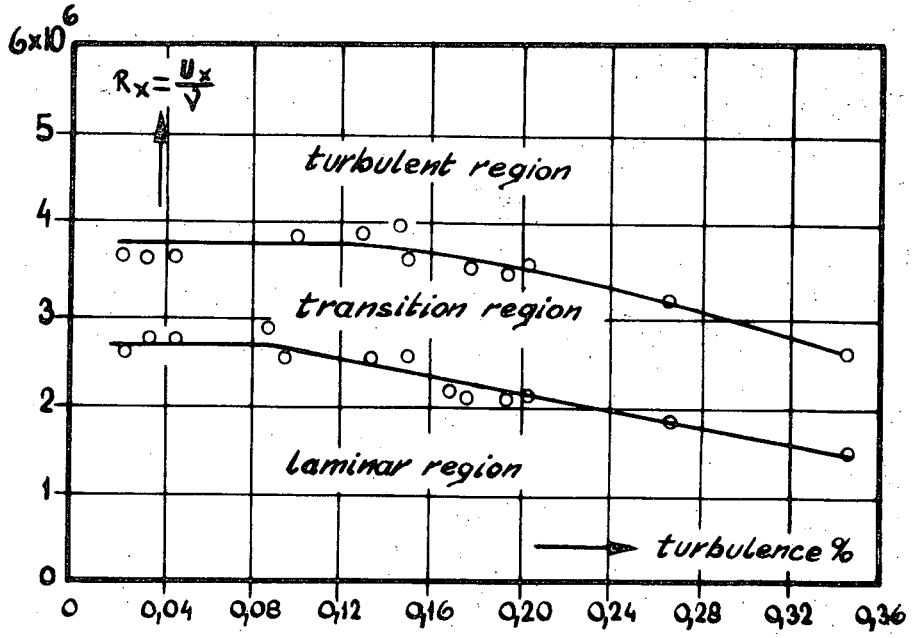

Fig.2: Effect of turbulence on x-Reynoldsnumber for transition of boundary layer along flat plate (NACA Report 909)

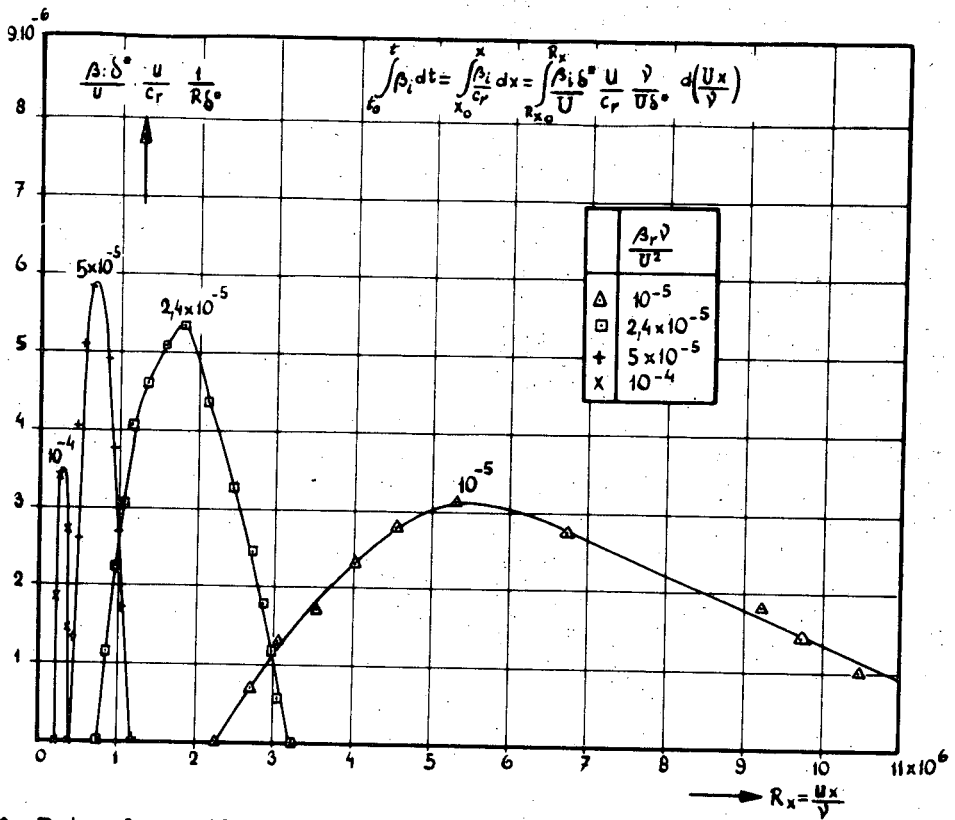

Fig.3: Rate of amplification for oscillations in the laminar boundary layer along flat plate.

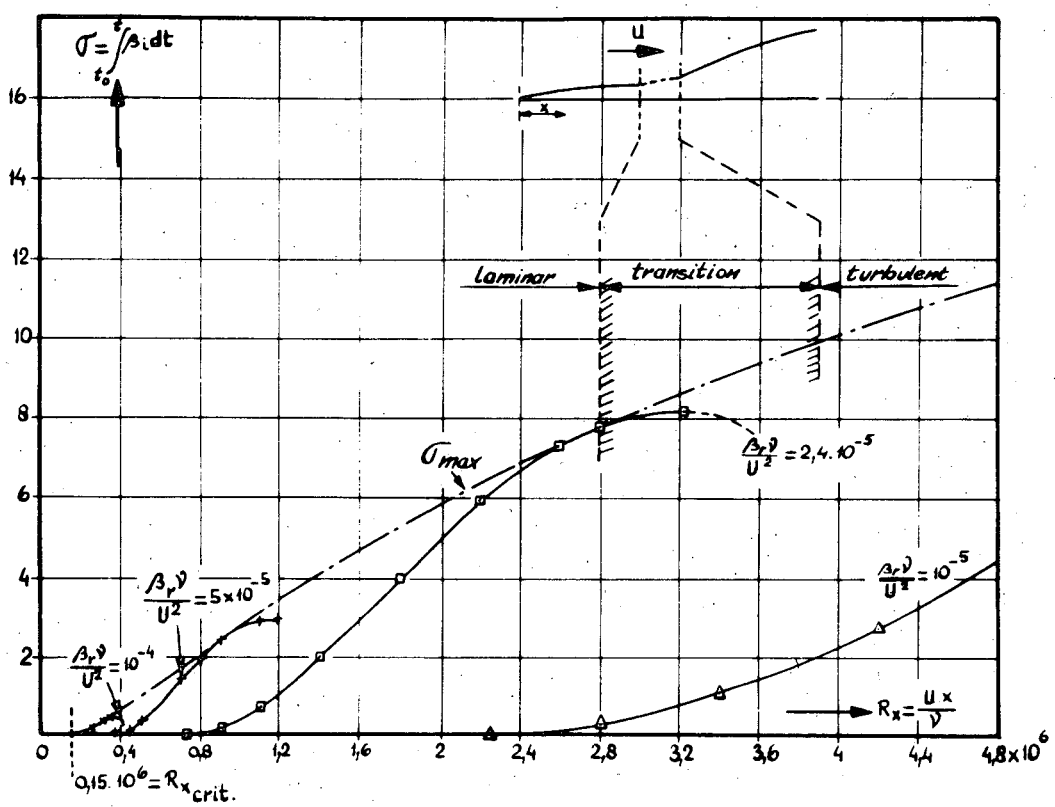

Fig.4: Amplification factor for oscillations in laminar boundary-layer along flat plate.

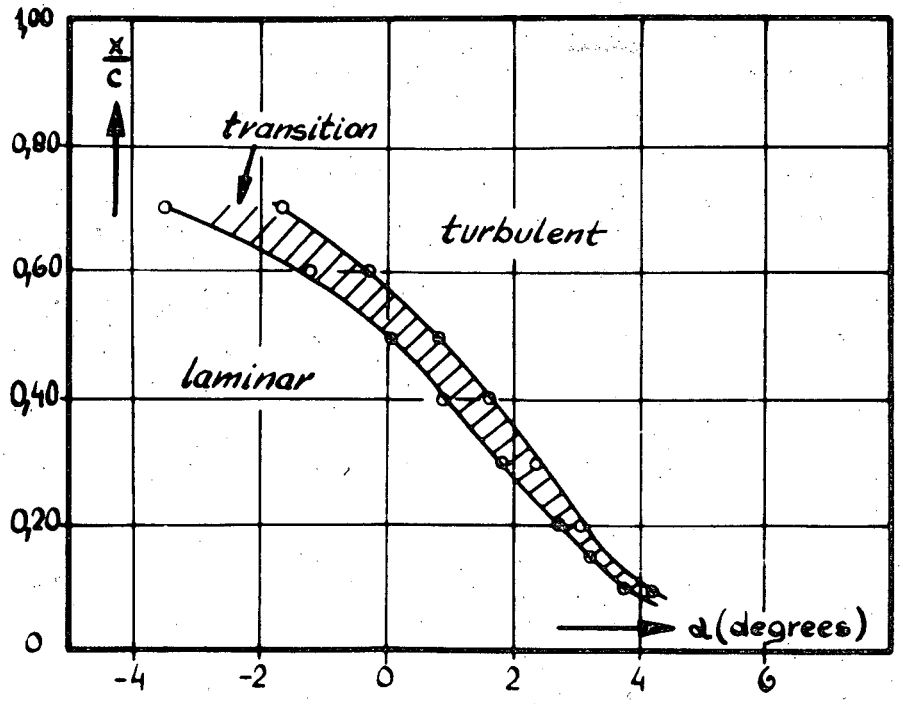

Fig.5: Transition region, EC 1440 airfoil section; $R = 4{,}35 \times 10^6$.

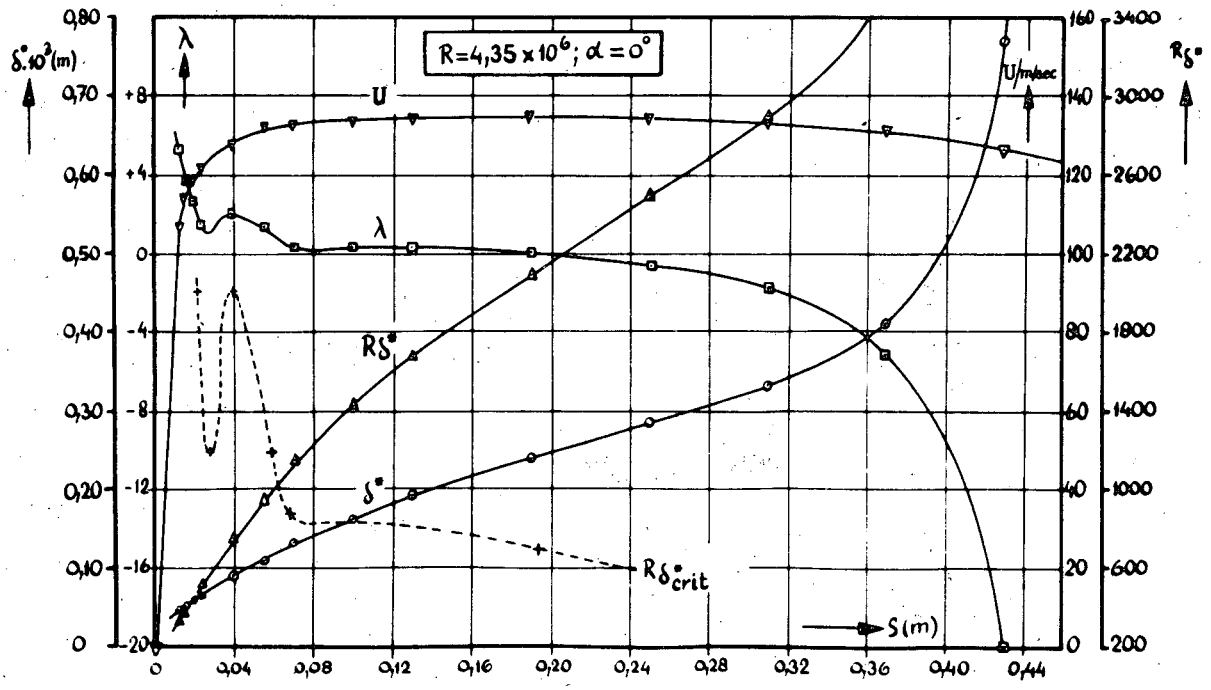

Fig.6: Results of the boundary layer calculations for the EC 1440 airfoil section.

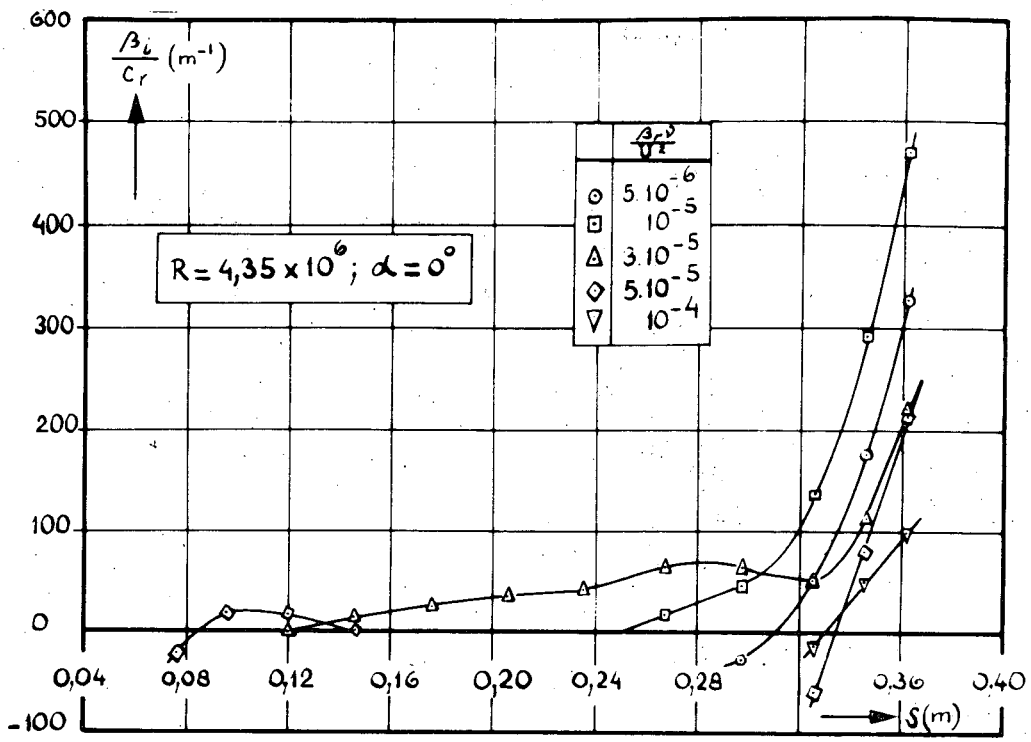

Fig.7: Rate of amplification for oscillations in the laminar boundary layer of the airfoil section EC 1440.

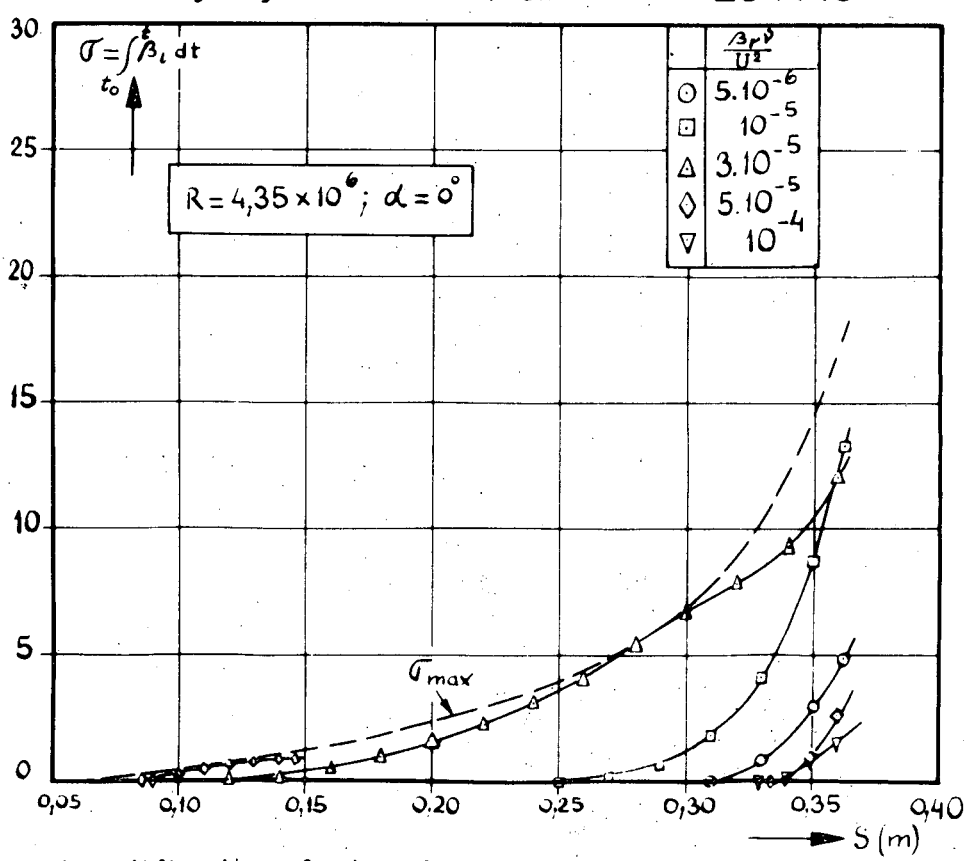

Fig.8: Amplification factor for oscillations in the laminar boundary layer of the EC 1440 airfoil section.

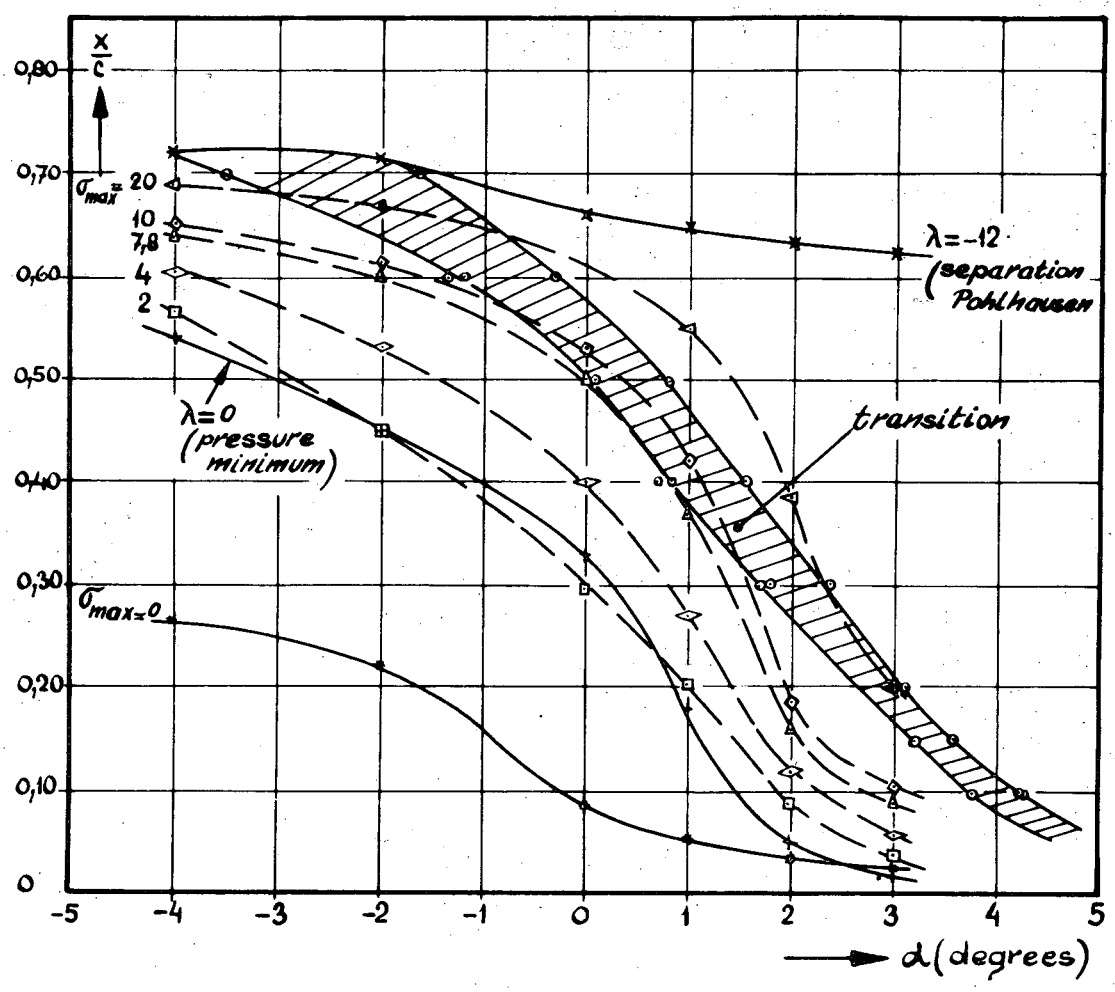

Fig.9: Calculated amplification factor and measured transition region for the EC 1440 airfoil section

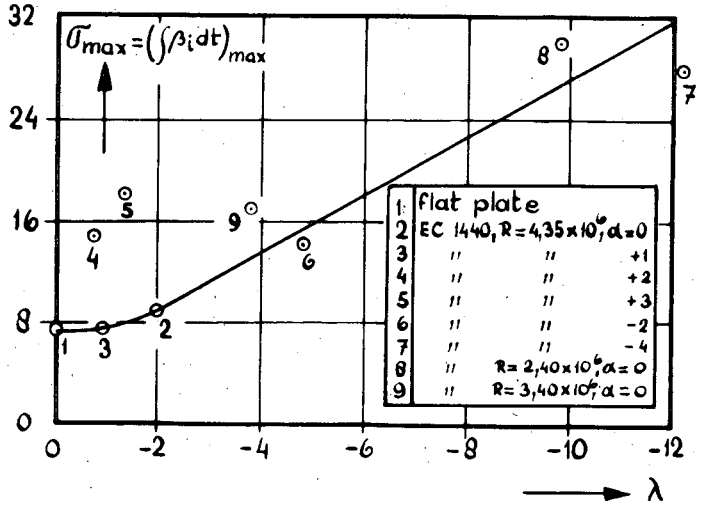

Fig.10: Maximum amplification factor at beginning of transition region as a function of λ.